

On a model for continuous sedimentation in vessels with discontinuous cross-sectional area

R. Bürger¹, K. H. Karlsen², N. H. Risebro³, and J. D. Towers⁴

¹ Institute of Mathematics A, University of Stuttgart
Pfaffenwaldring 57, D-70569 Stuttgart, Germany.
E-mail: buerger@mathematik.uni-stuttgart.de

² Department of Mathematics, University of Bergen,
Johs. Brunsgt. 12, N-5008 Bergen, Norway. E-Mail: kennethk@mi.uib.no

³ Department of Mathematics, University of Oslo,
P.O. Box 1053, Blindern, N-0316 Oslo, Norway. E-Mail: nilshr@math.uio.no

⁴ MiraCosta College, 3333 Manchester Avenue,
Cardiff-by-the-Sea, CA 92007-1516, USA. E-Mail: jtowers@cts.com

Summary. We study a clarifier-thickener unit considering that its cross-sectional area is not constant in both the clarification and the thickening zones. A mathematical model of sedimentation in such a vessel can be formulated as an initial value problem for a scalar conservation law with a nonconvex spatially varying flux and several types of discontinuities with respect to the space variable. Weak solutions of this non-standard conservation law are approximated by an extension of the well-known Engquist-Osher scheme. The key new ingredient is the discretization of the discontinuous flux parameters on a grid staggered against that of the conserved (sought) variable. The mathematical model and the numerical scheme are illustrated by a number of simulations.

1 Introduction

The kinematic theory of one-dimensional sedimentation of ideal suspensions originated in Kynch's paper [26]. Its main assumption states that in a suspension of small equal-sized solid particles dispersed in a viscous fluid, considered as a superposition of two continuous phases, the solid-fluid relative or slip velocity v_r is a function of the local solids concentration u only. Under this assumption and defining the so-called Kynch batch flux density function $h(u) := u(1-u)v_r(u)$, we can state the governing equation for batch settling of a suspension in a cylindrical closed vessel as the scalar conservation law $u_t + h(u)_x = 0$. The function $h(u)$ depends on the material specific properties of the mixture under study. A very frequently used function is [30]

$$h(u) = v_\infty u(1-u)^n, \quad v_\infty > 0, \quad n \geq 1, \quad (1)$$

where $v_\infty > 0$ is the settling velocity of a single particle in an unbounded pure fluid. It should be pointed out that the kinematic sedimentation model forms an example of the general theory of kinematic waves by Lighthill and Whitham [28, 34], and is very similar to the kinematic theory of traffic flow on highways. It soon turned out that the kinematic wave theory bears severe

shortcomings in the practical application to traffic flow, which essentially are due to the fact that cars equipped with anisotropic ‘driver psychology’ can not simply be described as a flowing continuum. This led to the (apparently, still controversial [16]) postulation of additional ‘momentum’ equations [2, 21]. On the other hand, numerous studies (see [10, 11] for overviews) and extensive use in industry have established the kinematic sedimentation theory as a useful description for the settling of a variety of materials such as mineral tailings, wastewater and blood. Due to its simplicity, the traffic flow model is used in many textbooks as an instructive applicative example for a nonlinear scalar conservation law. However, the application of the same equation (but with a non-convex flux) to sedimentation of suspensions has gained more practical importance.

In its ‘raw’ form, the equation $u_t + h(u)_x = 0$ applies to batch settling in a closed column. Practitioners very soon used the kinematic sedimentation theory for design calculations of continuously operated settling tanks, so-called thickeners, by adding a transport term $q(t)u$ to the flux density function $h(u)$, where $q(t)$ is a controllable mixture flow velocity [22, 32]. This results in the equation

$$u_t + (q(t)u + h(u))_x = 0. \quad (2)$$

Several researchers recognized that information on whether a cylindrical continuous thickener is able to treat a given suspension with a known function $h(u)$ under stationary flow conditions can essentially be read off from plots of the continuous flux function $qu + h(u)$ (with $q = q(t)$ kept constant) [23, 24, 31, 35]. However, to use (2) for the simulation of continuous sedimentation, one needs to explicitly model the feed and discharge mechanisms and to provide (in the widest sense) boundary conditions. At the latest at this point engineering intuition had to give way to serious mathematical analysis.

Petty [29] was the first to propose Dirichlet boundary concentrations for Eq. (2), but recognized that the resulting model was not well-posed since overflow and underflow concentration waves may break through the feed and discharge boundary levels, such that in dependence of the solution u , prescribed boundary data are ignored. The well-posedness of a scalar conservation law with boundary conditions was recovered by the concept of (set-valued) entropy boundary conditions developed by Bardos et al. [3], Dubois and Le Floch [19] and Le Roux [27]. In a series of papers, Bustos and her co-workers utilized this new concept to provide a rigorous mathematical framework to continuous sedimentation, including existence and uniqueness results [14] and constructions of elementary solutions [12] and a control model [13].

In spite of its amenability to mathematical analysis, the Petty-Bustos model [12, 13, 14, 29] suffers from some drawbacks. Among them is the lack of a global conservation principle due to the use of Dirichlet boundary conditions, and the complete neglect of a clarification zone. It is preferable to replace the Dirichlet boundary conditions by transitions between the transport flux $q(x, t)u$ and the composite flux $q(x, t)u + h(u)$, which leads to a

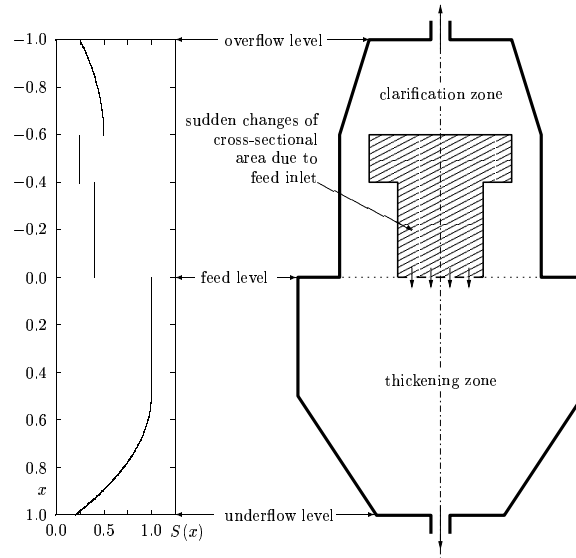


Fig. 1. Vertical cross-section of an axisymmetric clarifier-thickener unit characterized by its cross-sectional area function $S(x)$.

pure initial value problem. Moreover, the feed suspension should enter *between* the overflow outlet at the top and the discharge outlet at the bottom. This gives rise to an upwards-directed volume average velocity $q_l \leq 0$ above and a downwards-directed velocity $q_r \geq 0$ below the feed level. The feed source itself is modeled by a singular source term.

Thorough constructions and classifications of solutions of clarifier-thickener models were presented in a series of papers by Diehl, see [17, 18] and the references cited therein. We have adopted a more computational approach and are interested in devising numerical methods for clarifier-thickener units for proving existence of weak solutions and to provide a simulation tool. Thereby we can also include a quasi-one-dimensional formulation of a vertical vessel with a variable cross-sectional area $S(x)$, where $-1 \leq x \leq 1$ is the dimensionless depth variable. For such a configuration it is at least complicated [1] to construct exact solutions by the method of characteristics. Within our finite differencing framework, it is not even necessary to assume that $S(x)$ is a continuous function of depth x , i.e. we allow $S(x)$ to have jumps. Such jumps occur, for example, at the feed level due to the internal feed mechanism, see Figure 1.

The remainder of the paper is organized as follows. In Section 2 the governing equation for continuous sedimentation in a vessel with varying cross section is derived in some detail. In the formulation of the final initial value problem we add the feed source to the model for constant cross-sectional area formulated in [6, 7, 8]. Moreover, weak solutions are defined and the main

convergence result is stated. In Section 3 the numerical method is outlined and its basic properties are stated. In Section 4 we present (and discuss) numerical examples in the application to clarifier-thickener models.

2 Mathematical model

We assume that $x = -1$ is the overflow level, $x = 0$ corresponds to the feed level and $x = 1$ is the discharge level, and assume that the unknown volumetric solids concentration u depends on depth only, i.e., $u = u(x, t)$. Then the conservation of mass equations for the solids and the fluid are

$$S(x)u_t + (S(x)uv_s)_x = 0, \quad (3)$$

$$-S(x)u_t + (S(x)(1-u)v_f)_x = 0, \quad (4)$$

respectively, where t is time and v_s and v_f are the solids and the fluid phase velocities. The mixture flux, that is the volume average flow velocity weighted with $S(x)$, is given by $Q(x, t) := S(x)(uv_s + (1-u)v_f)$.

The sum of (3) and (4) produces the continuity equation of the mixture, $Q_x = 0$ for $-1 < x < 0$ and $0 \leq x \leq 1$ and $t > 0$, which implies that $Q(\cdot, t)$ is constant as a function of x . Since Q only suffers a jump across the feed source level $x = 0$, we get for $t > 0$

$$Q(x, t) = \begin{cases} Q(-1, t) = Q_L(t) & \text{for } -1 \leq x < 0, \\ Q(1, t) = Q_R(t) & \text{for } 0 < x \leq 1, \end{cases} \quad (5)$$

where $Q_L(t) \leq 0$ and $Q_R(t) \geq 0$ are the signed volumetric suspension overflow and discharge rates, respectively, prescribed by the control of the suspension volume flows at $x = -1$ and $x = 1$. Note that we here identify a downwards flow with a flow to the right. Equation (5) is equivalent to one of the mass balance equations. We let (5) replace (4) and rewrite (3) in terms of the flow rate $Q(x, t)$ and the solid-fluid relative velocity or slip velocity $v_r := v_s - v_f$, for which a constitutive equation will be formulated. Observing that

$$uv_s = (uv_s + (1-u)v_f)u + u(1-u)(v_s - v_f) = \frac{Q(x, t)u}{S(x)} + u(1-u)v_r, \quad (6)$$

and assuming for a moment that no solids enter the vessel at $x = 0$, we obtain from (3) $S(x)u_t + (Q(x, t)u + S(x)u(1-u)v_r)_x = 0$. Expressing v_r in terms of $h(u)$, we arrive at $S(x)u_t + (Q(x, t)u + S(x)h(u))_x = 0$. The function h is assumed to be piecewise differentiable with $h(u) = 0$ for $u \leq 0$ or $u \geq u_{\max}$, where u_{\max} is the maximum solids concentration, $h(u) > 0$ for $0 < u < u_{\max}$, $h'(0) > 0$ and $h'(u_{\max}) \leq 0$. For simplicity we assume that $u_{\max} = 1$.

For the analysis we assume that $h \in C^2[0, 1]$, and that h is genuinely non-linear in the sense that $|h''| > 0$ except for finitely many inflection points. Several authors have studied one-dimensional sedimentation in non-cylindrical

vessels [1, 5, 15, 17, 33] under the assumption that S is a smooth function of x . We here assume that S is only piecewise continuous, which means that the diameter jumps. In this case the available mathematical and numerical theory breaks down. We assume that $0 < S_{\min} \leq S(x) \leq S_{\max}$ for $x \in \mathbf{R}$ and $|S|_{BV} < \infty$, and that the initial data u_0 satisfies $u_0 \in L^1(\mathbf{R}) \cap BV(\mathbf{R})$, $0 \leq u_0(x) \leq 1$ for $x \in \mathbf{R}$. To simplify the problem further, we assume $Q_L(t) = Q_L = \text{Const.}$ and $Q_R(t) = Q_R = \text{Const.}$ As in [6, 7], we assume that at $x = 1$, the composite flux $Q_R u + S(x)h(u)$ is changed to the discharge transport flux $Q_R u$, and that at $x = 0$, a feed source is located. To model this feed source, we recall that a clarifier-thickener unit with $S \equiv S_0 = \text{const.}$ can be modeled by the equation $u_t + \hat{g}(u, x)_x = 0$ with the composite flux

$$\hat{g}(u, x) = \begin{cases} q_L u & \text{for } x < -1, \\ q_R u + h(u) + (q_R - q_L)u_F & \text{for } 0 < x < 1, \\ q_L u + h(u) & \text{for } -1 < x < 0, \\ q_R u + (q_L - q_R)u_F & \text{for } x > 1, \end{cases}$$

where $q_L = Q_L/S_0 \leq 0$ and $q_R = Q_R/S_0 \geq 0$ are the prescribed volume overflow and discharge rates, respectively, divided by the cross-sectional area, and $u_F \in [0, u_{\max}]$ is the concentration of the suspension fed into the unit through the singular source at $x = 0$ at the volumetric rate $Q_F = Q_R - Q_L$. Subtracting the constant term $(q_L - q_R)u_F$ from the flux $\hat{g}(u, x)$, we can finally state our problem as the initial-value problem

$$S(x)u_t + g(u, x)_x = 0, \quad x \in \mathbf{R}, \quad t > 0, \quad (7a)$$

$$g(u, x) = Q_R u_F + \begin{cases} Q_L(u - u_F) & \text{for } x < -1, \\ Q_L(u - u_F) + S(x)h(u) & \text{for } -1 < x < 0, \\ Q_R(u - u_F) & \text{for } x > 1, \\ Q_R(u - u_F) + S(x)h(u) & \text{for } 0 < x < 1, \end{cases} \quad (7b)$$

$$u(x, 0) = u_0(x), \quad x \in \mathbf{R}; \quad u_0(x) \in [0, u_{\max}] \quad \text{for all } x. \quad (7c)$$

Independently of the smoothness of $g(u, \cdot)$ and of u_0 , solutions of (7b)–(7c) are in general discontinuous, and so weak solutions must be sought.

Definition 1. A bounded measurable function $u(x, t)$ is a weak solution of (7) if for all test functions $\phi \in \mathcal{D}(\Pi_T)$ such that $\phi|_{t=T} = 0$,

$$\iint_{\Pi_T} (S(x)u\phi_t + g(u, x)\phi_x) dx dt + \int_{\mathbf{R}} u_0(x)\phi(x, 0)S(x) dx = 0. \quad (8)$$

Our latest result, which is proved in [9], is stated in the following theorem:

Theorem 1. There exists a weak solution to (7), and this weak solution can be constructed as a limit of a sequence of approximate solutions constructed by a finite difference scheme.

3 Numerical method

To facilitate the notation and analysis, we define the composite flux function $f(\gamma(x), u) := g(u, x)$, where $\gamma(x) := (\gamma_1(x), \gamma_2(x))$ is the vector of the flux parameters $\gamma_1(x) := S(x)\chi_{[-1,1]}(x)$ and $\gamma_2(x) := Q_L$ for $x < 0$ and $\gamma_2(x) := Q_R$ for $x > 0$. In this notation, we have $f(\gamma, u) = \gamma_2(u - u_F) + \gamma_1 h(u) + Q_R u_F$. Thus the initial value problem for the conservation law (7b) reads

$$S(x)u_t + f(\gamma(x), u)_x = 0, \quad u(x, 0) = u_0(x). \quad (9)$$

We now define a numerical method for (9). We choose a discretization Δx , Δt , set $x_j := j\Delta x$, $t^n := n\Delta t$, and then discretize the coefficient vector γ , the initial data, and the cross sectional area by setting

$$\gamma_{j+\frac{1}{2}} = \frac{1}{\Delta x} \int_{x_j}^{x_{j+\frac{1}{2}}} \gamma(x) dx, \quad U_j^0 = \frac{1}{\Delta x} \int_{x_{j-\frac{1}{2}}}^{x_{j+\frac{1}{2}}} u_0(x) dx, \quad S_j = \frac{1}{\Delta x} \int_{x_{j-\frac{1}{2}}}^{x_{j+\frac{1}{2}}} S(x) dx.$$

Let Δ_- and Δ_+ denote backward and forward spatial difference operators. For $n > 0$ we define $U_j^n \approx u(x_j, t^n)$ by the explicit marching formula

$$U_j^{n+1} = U_j^n - \lambda_j \Delta_- f^{\text{EO}}(\gamma_{j+\frac{1}{2}}, U_{j+1}^n, U_j^n), \quad (10)$$

where $\lambda_j = \Delta t / (S_j \Delta x)$, and f^{EO} is defined by

$$f^{\text{EO}}(\gamma, v, u) = \frac{1}{2} \left(f(\gamma, u) + f(\gamma, v) - \int_u^v |f_u(\gamma, w)| dw \right), \quad (11)$$

which is a slight generalization of the standard Engquist-Osher flux [20].

An important feature of our scheme is that the discretization of the parameter vector γ is *staggered* with respect to that of the conserved variable u . This greatly simplifies both the scheme and its analysis. Were the two discretizations aligned, more complicated 2×2 Riemann problems would have to be solved. Mesh staggering allows us to use a simple scalar Riemann solver.

Our choice of the Engquist-Osher Riemann solver is motivated by two considerations. First, it results in an upwind scheme, allowing for relatively sharp resolution of discontinuities. Second, the Engquist-Osher flux has a close functional relationship with a certain singular mapping to be introduced below, which has enabled us to prove convergence (along a subsequence) of the approximate solutions generated by the scheme. The following lemma, proved in [9], summarizes some important properties of our difference scheme.

Lemma 1. *Let $f_u^+(w) = \max(f_u(w), 0)$, $f_u^-(w) = \min(f_u(w), 0)$. If the ratio $\Delta x / \Delta t$ is chosen so that the following CFL condition is satisfied*

$$\lambda_j |f_u^+(\gamma_{j+\frac{1}{2}}, U_j^n) - f_u^-(\gamma_{j-\frac{1}{2}}, U_j^n)| \leq 1, \quad \forall j \in \mathbf{Z}, \quad (12)$$

then the computed solutions remain in the interval $[0, 1]$, the CFL condition (12) holds for each succeeding time step, and the scheme (10) is monotone. In addition, there exists a constant C , independent of Δ , such that

$$\sum_{j \in \mathbf{Z}} |U_j^{n+1} - U_j^n| S_j \Delta x \leq \sum_{j \in \mathbf{Z}} |U_j^1 - U_j^0| S_j \Delta x \leq C \Delta t.$$

Let χ^n denote the characteristic function of $[t_n, t_{n+1})$ and χ_j the characteristic function of $[x_{j-\frac{1}{2}}, x_{j+\frac{1}{2}})$. We then define

$$u^\Delta(x, t) := \sum_{n \geq 0} \sum_{j \in \mathbf{Z}} U_j^n \chi_j(x) \chi^n(t), \quad \text{and} \quad \gamma^\Delta(x) := \sum_{j \in \mathbf{Z}} \gamma_{j+\frac{1}{2}} \chi_{j+\frac{1}{2}}(x).$$

As mentioned above, our main result is convergence of a subsequence of the approximations u^Δ to a weak solution u of the conservation law. The key ingredient in the proof is the use of a so-called singular mapping, defined by $\Psi(\gamma, u) := \int_0^u |f_u(\gamma, w)| dw$. For these problems, a bound on the total variation of the conserved quantity u is very difficult, if not impossible, which makes it necessary to use the singular mapping approach. We transform the numerical approximations according to $z^\Delta = \Psi(\gamma^\Delta, u^\Delta)$, and prove compactness for the transformed sequence z^Δ . Since Ψ is continuous and strictly increasing in its second argument, it is possible to recover the limit of the conserved variable u by inverting Ψ . The scheme also satisfies a set of cell entropy inequalities. For limit solutions that are piecewise smooth, it follows from the results in [25] that certain geometric entropy conditions are satisfied, and that such solutions form an L^1 contraction semigroup.

4 Numerical examples

The physical problem and the finite difference scheme from Section 3 are now illustrated by some numerical examples. As in [4, 5], we assume that the function h is given by (1) with $v_\infty = 1$ and $n = 5$. Here, we let a clarifier-thickener unit be defined by the dimensionless function (see Figure 1)

$$S(x) = \begin{cases} 0.5 - 1.5625(x + 0.6)^2 & \text{for } x \in (-1, -0.6], \\ 0.25 & \text{for } x \in (-0.6, -0.4], \\ 0.5 & \text{for } x \in (-0.4, 0], \\ 1 & \text{for } x \in (0, 0.5], \\ 1 - 3.2(x - 0.5)^2 & \text{for } x \in (0.5, 1). \end{cases}$$

In the numerical examples (see Figure 2) we use $\Delta x = 1/100$ and $\lambda = 0.05$. Note that the computational grid is finer than the visual grid used to display the results. The four cases correspond to different parameters Q_L , Q_R and u_F , which are chosen as constants (with respect to t) and produce different modes

of behavior of the clarifier-thickener unit. See [18] for detailed analytical predictions of the clarifier-thickener response to operating conditions.

The first case (Figure 2 upper left) corresponds to $Q_L = -0.1$, $Q_R = 0.1$ and $u_F = 0.4$. The simulation shows that the solids initially settle exclusively into the thickening zone ($x > 0$) and form a rising sediment, which breaks through the feed level ($x = 0$) at about $t = 20$. The particles entering the clarification zone ($x < 0$) start to produce an overflow of clarified suspension at about $t = 29$. The shape of the concentration surface in that zone reflects the vessel geometry, and that there the solution becomes stationary. The system converges to a steady state of simultaneous clarification and thickening.

The second case (Figure 2 upper right) is produced by $Q_L = -0.1$, $Q_R = 0.4$ and $u_F = 0.4$. This choice again leads to a steady state, but the solids immediately start at $t = 0$ to enter the clarification zone.

The third case (Figure 2 lower left) corresponds to $Q_L = -0.2$, $Q_R = 0.0$ and again $u_F = 0.4$, i.e. the vessel is kept closed at its bottom. Thus, the thickening zone is slowly filled up. Moreover, as in the second example, particles start immediately to enter the clarification zone. An additional solids flux into that zone is produced when the rising sediment reaches the feed level. This leads to an increase of the concentrations in the clarification zone, which in contrast to the first and second case does not remain stationary.

In the first three examples, the solution at large times reflects the vessel geometry. This is not valid in the fourth case (Figure 2 lower right), where we apply a strong feed flux by letting $Q_L = -0.2$, $Q_R = 0.2$ and $u_F = 0.8$. In this ‘hydraulic forcing’ situation, the feed slurry immediately breaks into the clarification zone, which it leaves undiluted. The thickening zone first fills up successively, with a dilution of the feed suspension and sediment forming, but then also replenishes with the feed slurry at its feed concentration.

References

1. Anestis, G. (1981): Eine eindimensionale Theorie der Sedimentation in Absetzbehältern veränderlichen Querschnitts und in Zentrifugen. Doctoral Thesis, Technical University of Vienna, Austria.
2. Aw, A. (2000): Resurrection of “second order” models of traffic flow. *SIAM J. Appl. Math.* **60**, 916–938.
3. Bardos, C., Le Roux, A.Y. and Nedelec, J.C. (1979): First order quasilinear equations with boundary conditions. *Comm. Partial Diff. Eqs.* **4**, 1017–1034.
4. Bürger, R., Concha, F. (2001): Settling velocities of particulate systems: 12. Batch centrifugation of flocculated suspensions. *Int. J. Mineral Process.* **63**, 115–145
5. Bürger, R., Damasceno, J.J.R., Karlsen, K.H. (2001): A mathematical model for batch and continuous thickening in vessels with varying cross section, Preprint 2001/11, SFB 404, University of Stuttgart.
6. Bürger, R., Karlsen, K.H., Klingenberg, C., Risebro, N.H. (2002): A front tracking approach to a model of continuous sedimentation in ideal clarifier-thickener units. *Nonlin. Anal. Real World Appl.*, to appear.

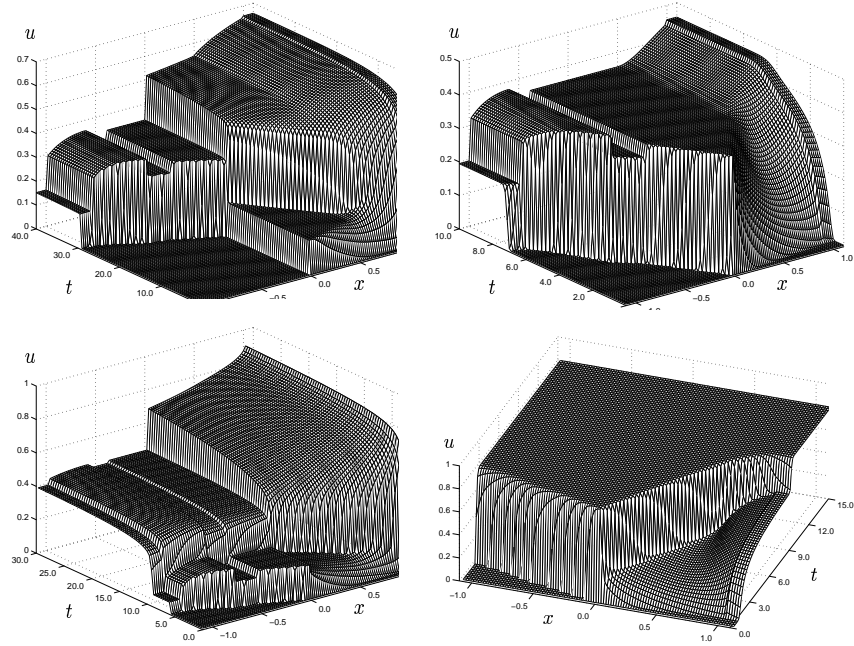


Fig. 2. Simulation of the operation of the continuous clarifier-thickener.

7. Bürger, R., Karlsen, K.H., Risebro, N.H., Towers, J.D. (2001): Numerical methods for the simulation of continuous sedimentation in ideal clarifier-thickener units. Preprint, University of Bergen.
8. Bürger, R., Karlsen, K.H., Risebro, N.H., Towers, J.D. (2002): Convergence of a difference scheme for continuous sedimentation in ideal clarifier-thickener units. In preparation.
9. Bürger, R., Karlsen, K.H., Risebro, N.H., Towers, J.D. (2002): Monotone difference approximations for the simulation of clarifier-thickener units. Submitted to Comp. Visual. Sci.
10. Bürger, R. and Wendland, W.L. (2001): Sedimentation and suspension flows: Historical perspective and some recent developments. *J. Eng. Math.* **41**, 101–116.
11. Bustos, M.C., Concha, F., Bürger, R., Tory, E.M. (1999): *Sedimentation and Thickening*. Kluwer Academic Publishers, Dordrecht, The Netherlands.
12. Bustos, M.C., Concha, F. and Wendland, W.L. (1990): Global weak solutions to the problem of continuous sedimentation of an ideal suspension, *Math. Meth. Appl. Sci.* **13**, 1–22.
13. Bustos, M.C., Paiva, F. and Wendland, W.L. (1990): Control of continuous sedimentation of ideal suspensions as an initial and boundary value problem, *Math. Meth. Appl. Sci.* **12**, 533–548.
14. Bustos, M.C., Paiva, F. and Wendland, W.L. (1996) Entropy boundary conditions in the theory of sedimentation of ideal suspensions. *Math. Meth. Appl. Sci.* **19**, 679–697.

15. Chancelier, J.P., Cohen de Lara, M., Joannis, C., Pacard, F. (1997): New insights in dynamic modeling of a secondary settler—I. Flux theory and steady-states analysis. *Wat. Res.* **31**, 1847–1856.
16. Daganzo, C.F. (1995): Requiem for second-order fluid approximations of traffic flow, *Transp. Res. B* **29B**, 277–286.
17. Diehl, S. (1997): Dynamic and steady-state behavior of continuous sedimentation. *SIAM J. Appl. Math.* **57**, 991–1018.
18. Diehl, S. (2001): Operating charts for continuous sedimentation I: Control of steady states. *J. Eng. Math.* **41**, 117–144.
19. Dubois, F. and Le Floch, P. (188): Boundary conditions for non-linear hyperbolic systems of conservation laws, *J. Diff. Eqns.* **71**, 93–122.
20. Engquist, B. and Osher, S. (1980): Stable and entropy-satisfying approximations for transonic flow calculations. *Math. Comp.* **34**, 45–75.
21. Greenberg, J.M. (2001): Extensions and amplifications of a traffic model of Aw and Rascle. *SIAM J. Appl. Math.* **62**, 729–745.
22. Hassett, N.J. (1958): Design and operation of continuous thickeners. *Ind. Chemist* **34**, 116–120, 169–172, 489–494.
23. Hassett, N.J. (1964/65): Mechanism of thickening and thickener design. *Inst. Min. Met. Trans.* **74**, 627–656.
24. Hassett, N.J. (1968): Thickening in theory and practice, *Min. Sci. Eng.* **1**, 24–40.
25. Karlsen, K.H., Risebro, N.H., Towers, J.D. (2002): L^1 stability for piecewise smooth entropy solutions of nonlinear degenerate parabolic convection-diffusion equations with discontinuous coefficients. In preparation.
26. Kynch, G.J. (1952): A theory of sedimentation. *Trans. Farad. Soc.* **48**, 166–176.
27. Le Roux, A.Y. (1977): Etude du problème mixte pour une équation quasi-linéaire du premier ordre, *C. R. Acad. Sci. Paris Sér. A* **285**, 351–354.
28. Lighthill, M.J. and Whitham, G.B. (1955): On kinematic waves: I. Flood movement in long rivers, II. A theory of traffic flow on long crowded roads, *Proc. Royal Soc. A* **229**, 281–316 and 317–345.
29. Petty, C.A. (1975): Continuous sedimentation of a suspension with a nonconvex flux law. *Chem. Eng. Sci.* **30**, 1451–1458.
30. Richardson, J.F. and Zaki, W.N. (1954): Sedimentation and fluidization: Part I. *Trans. Instn. Chem. Engrs. (London)* **32**, 35–53.
31. Shannon, P.T. and Tory, E.M. (1966): The analysis of continuous thickening. *SME Trans.* **235**, 375–382.
32. Talmage, W.P. and Fitch, E.B. (1955): Determining thickener unit areas. *Ind. Eng. Chem.* **47**, 38–41.
33. White, D.A. Verdone, N. (2000): Numerical modelling of sedimentation processes. *Chem. Eng. Sci.* **55**, 2213–2222.
34. Whitham, G.B. (1974): *Linear and Nonlinear Waves*. Wiley, New York.
35. Yoshioka, N., Hotta, Y., Tanaka, S., Naito, S. and Tsugami, S. (1957): Continuous thickening of homogeneous flocculated slurries. *Chem. Engrg. Japan* **21**, 66–75.